Epitope mapping by photobleaching fluorescence resonance energy transfer measurements using a laser scanning microscope system

Gàbor Szabò Jr.,* P. Scott Pine, James L. Weaver, Mark Kasari, and Adorjan Aszalos
Center for Drug Evaluation and Research, Food and Drug Administration, 200 C St. SW, Washington, DC 20204 USA; and
*Department of Biophysics, University Medical School of Debrecen, 4012 Debrecen, Hungary

ABSTRACT The donor photobleaching method (T. M. Jovin and D. J. Arndt-Jovin. 1989. *Annu. Rev. Biophys. Biophys. Chem.* 18:271–308.) has been adapted to an ACAS 570 (laser scanning microscope) system to measure fluorescence resonance energy transfer (FRET) on individual human peripheral blood T cells. Photobleaching was completed in ~100 ms in our case and it followed double-exponential kinetics. The energy transfer efficiency (E) was ~20% between the CD4 epitopes OKT4-FITC and Leu-3a-PE as well as between OKT4E-FITC and OKT4-PE. E was ~8% between OKT4-FITC and Leu-4-PE (αCD3) and barely detectable (~4%) from OKT4-FITC to Leu-5b-PE (αCD2). The E values obtained by the photobleaching method were highly reproducible both in repeated measurement of identical samples and in experiments with different batches of cells and were in agreement with the flow cytometric donor quenching measurements. As expected, E measured between primary and secondary layers of antibodies increased (from ~14% to ~28%) when $F(ab')_2$ fragments were substituted for whole antibody molecules as the donor. On a T cell line we mapped the distance between the idiotypic determinant of the T cell receptor (TcR) and the Leu-4 epitope of CD3 as proximal as E = 28%, as compared to E = 4% between a framework TcR epitope and Leu-4. In the latter case, however, ~40% less Leu-4 was bound suggesting that the antigen binding site of TcR is in close proximity with one of the two CD3 ε chains, which hence are not equivalent.

INTRODUCTION

Proximity measurements by fluorescence resonance energy transfer (FRET) methods on cell surfaces (reviewed, 1, 2) have gained an increasingly important role in the analysis of molecular interactions governing important cellular processes. The dependence of E (i.e., the ratio of FRET-related and combined deexcitation rates) on the average distance (R) between the donor (usually fluorescein) and the acceptor (mostly rhodamine) is described by the equation:

$$E = R^{-6}/(R^{-6} + R_0^{-6}) \quad (1)$$

for the simple case of a single donor-acceptor pair (R_0 is the distance where E is 50%). This extreme distance sensitivity of FRET makes it highly attractive for studying molecular conformation or intermolecular relationships. Quenching of the donor or sensitization of the acceptor fluorescence, corrected for differences in labeling and detection efficiencies and spectral spill overs are most commonly measured to assess E (1–3).

An alternate approach, introduced by Jovin and Arndt-Jovin (4) compares the photobleaching kinetics of the donor in the absence and presence of a proximal acceptor. This method is based on the observation that the integrated fluorescence in the course of complete bleaching is invariant to donor quantum efficiency and therefore is a true measure of the donor concentration actually present (5) and the view that the photochemical bleaching process involving the donor occurs from the excited singlet state. The rate constant of bleaching and the ratio of prebleach and integrated intensities were both used to calculate the transfer efficiency. Briefly reviewing their formulations:

$$E = 1 - T/T' = 1 - (I'_{d,0}/I'_{d,int})/(I_{d,0}/I_{d,int}) \quad (2)$$

where T and T' are the time constants of bleaching, $I_{d,0}$ and $I'_{d,0}$ are the initial fluorescence intensities, $I_{d,int}$ and $I'_{d,int}$ are the integrated intensities upon complete bleaching, in the absence and presence of an adequate acceptor, respectively; for derivation of the above equations (4–6). The availability of excited-state donors for photodestruction will decrease when this state is depleted by the presence of a proximal energy acceptor. Transfer will make photobleaching slower, starting from a quenched initial intensity with an unchanged integral. This method, "photobleaching FRET digital imaging microscopy" (pFRET) (4), offers greater sensitivity and an internal control for real donor concentration.

We have used this concept to develop a pFRET analysis routine on an ACAS 570 (stage scanning laser microscope) system, to control and extend our flow cytometric FRET measurements, applying a lifetime-related method. Using the ACAS for pFRET measure-

0006-3495/92/03/661/10 $2.00

ments has proved advantageous in that several thousands of time points can be recorded in the course of a very brief but complete photobleaching. This allowed an accurate analysis of the bleaching curves, with the initial intensity determined from an extrapolation based on the whole fitted curve, instead of a single measurement. Recently, Kubitscheck et al. (6) reported photobleaching FRET measurements of hapten binding to cell-bound IgE, using an experimental arrangement similar to ours. In their system, bleaching took several seconds (instead of ~0.1 s in our case) and the kinetics were approximated as a single exponential process, as opposed to the double-exponential kinetics we observed. We also introduced phycoerythrin (PE) as an energy acceptor, based on the large spectral overlap between fluorescein emission and PE absorption (7).

We have used this technique to study possible topological or conformational changes involving the T cell receptor (TcR)-CD3 complex and its ~55 kDa coreceptor, CD4, also the receptor for HIV (8–10). An obscure part in our understanding of the initial steps of T cell activation is a detailed knowledge of the molecular mechanics of changing conformation and topology of the receptors involved. Measuring actual distances on the cell surface with flow cytometric FRET technology proved to be a valuable tool in verifying proximity relationships of CD4. According to these findings (9) the TcR/CD3 complex and CD4 must properly associate for the T cell to be activated as part of the normal immune response. These results are confirmed and extended with further observations using our version of the photobleaching FRET method. We studied the spatial relationships between fluorochrome-labeled antibodies bound to various TcR/CD3 and CD4 antibody binding sites (epitopes). One of the αTcR antibodies used in our studies (WT31) is thought to bind to a framework epitope formed by both the α and β TcR chains; T40/25 (9) is specific for an idiotypic determinant of TcR on HPB-ALL; Leu-4 recognizes the ε chain of CD3. The αCD4 antibody Leu-3a recognizes the HIV gp120 binding site on the V1 domain of CD4 (most distal domain of this rodlike molecule relative to the cell membrane); OKT4E recognizes a discontinuous epitope on the same domain and OKT4 binds to a membrane-proximal epitope (8, 10). The distance between these epitopes could be subject to possible conformational changes upon T cell activation and gp120 binding or cross-linking. The present paper describes details of the ACAS-based photobleaching FRET method and data obtained on resting human peripheral blood (HPB) T cells and a leukemic T cell line, HPB-ALL (9).

MATERIALS AND METHODS

Cells and antibodies

Human peripheral blood lymphocytes derived from healthy donors were prepared by Ficoll-Hypaque centrifugation. The human T cell leukemia line HPB-ALL and a fluorescein isothiocyanate (FITC)-labeled anti-idiotypic αTcR antibody specific for this line were from Dr. D. B. Tse, Cornell University, Ithaca, New York. Cells were maintained in RPMI 1640 containing 2 mM glutamine (Gibco Laboratories, Grand Island, NY), supplemented with 10% Nu-serum (Collaborative Research Inc., Bedford, MA) and penicillin-streptomycin (Sigma Chemical Co., St. Louis, MO), for 1–5 d. The anti-CD4 (αCD4) antibodies used in our experiments were OKT4 (Ortho Diagnostics, Raritan, NJ) and OKT4E (a gift of Dr. P. Rao, Ortho Diagnostics) and Leu-3a (Becton Dickinson Microbiology Systems, Mountain View, CA). The other αTcR antibody used in our studies, αTcR-α/β-1 (clone WT31), was from Becton-Dickinson, as were Leu-4 (αCD3, ε-chain specific), Leu-5b (αCD2), and Leu-8. Anti-mouse IgG antibodies, whole and $F(ab')_2$ fragments, were from Sigma Chemical Co., as were the reagents FITC (isomer I) and R-phycoerythrin (PE). Streptavidin-PE, extravidin-TRITC, and allophycocyanin (APC) were from BD. Solutions of PE and FITC were used to calculate R_0, based on the normalized fluorescence spectrum of FITC and the absorption spectrum of PE (with a computer program that was kindly made available to us by Dr. J. R. Lakowicz, University of Maryland, Baltimore, MD). OKT4E was labeled with FITC to ~4 FITC/protein using standard methods titrated to label small quantities of antibody. Except for the OKT4E and the anti-idiotypic αTcR antibody, all other antibodies were commercially available in the conjugated forms described in Results.

Photobleaching

Photobleaching data collection for pFRET was performed on an ACAS 570 stage scanning laser (fluorescent) microscope (Meridian Instruments, Okemos, MI). The instrument is configured with a 5W argon laser and an Olympus OMT2 inverted microscope. The optical path is shown in Fig. 1. Treated cells were loaded in suspension into 15 μl Cunningham chamber slides and placed coverglass down on the microscope stage to use an Olympus 100× oil immersion objective lens, N.A. = 1.4. Cells (small lymphocytes in case of HPB samples) were positioned in the center of a 30-μm diameter laser illumination spot. The diameter of the laser at the plane of focus was determined by the knife-edge technique (11), and also checked by scanning fluorescent microbeads in line-scan mode and by observing the effective photobleaching area using a dense field of FITC-linked 6-μm beads (Becton Dickinson). The density of the cell suspension was such that neighboring cells were located outside the area to be bleached. The donor-only and the donor + acceptor samples were alternately bleached, with new slides prepared at every 10 cells. The argon laser was set for 100% of 1,000 mW at 488 nm. The effective power at the plane of focus was determined to be on the order of 10 mW using a power meter (Liconix, Santa Clara, CA) resulting in a power density of 1.4×10^3 W/cm^2. The beam diffuser provides a more even distribution of energy density within the photobleaching spot, but also contributes to a significant loss of power. Fluorescence intensity data, from the FITC channel (PMT1), were collected using the "point scan" mode of the ACAS Kinetics Analysis software (version 2.0 h). Each data point represents bleaching for a laser pulse width of 68 μs followed by a 20-ms interval. No emission (spectral spill-over) from PE-labeled antibody solution, in PBS or 1% formaldehyde, was detectable through the 520 ± 5-nm bandbass filter (used in the FITC channel of ACAS),

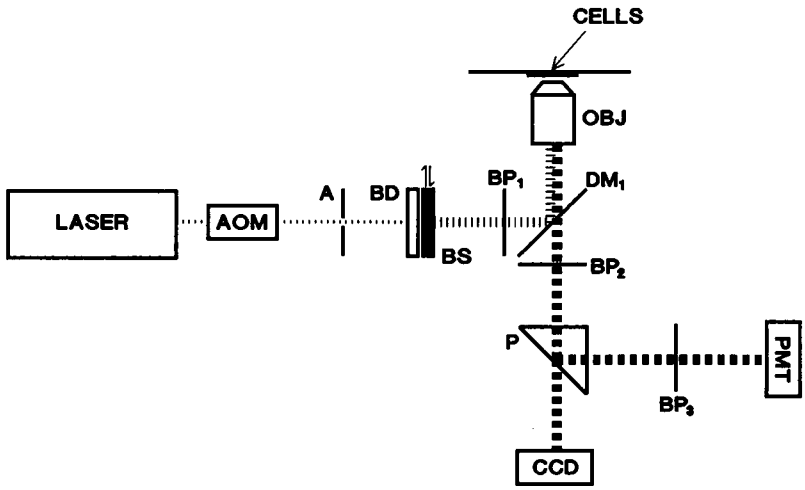

FIGURE 1 The 488-nm output of the laser is directed through an Acousto-Optic Modulator (AOM) which controls the intensity and pulse duration of the first-order beam. The first-order beam is selected with a pinhole aperture (A) and directed into the epi-illumination path of the microscope. A beam diffuser (BD) is used to expand the beam to illuminate an entire cell, followed by a moveable beam stop (BS) to block any laser light not regulated by the AOM (the BS is removed just before photobleaching). The beam then enters a standard Olympus fluorescence filter cube consisting of a 490 ± 10 nm bandpass filter (BP1), a 510-nm longpass dichroic mirror (DM_1), and 515-nm longpass filter (BP_2). The objective lens (OBJ, 100× oil, N.A. = 1.4) focuses the diffused beam to a spot size of 30 μm in diameter. The emitted fluorescence is then directed through a prism (P) which passes 20% of the signal to a CCD video camera and reflects 80% of the signal to the photomultiplier housing. The FITC signal is passed through a 520 ± 5-nm bandpass filter (BP_3) to be recorded by the PMT.

with excitation at 488 nm and emission scanned between 500–700 nm using a spectrofluorimeter (model MPF44A, Perkin Elmer Corp., Norwalk, CT).

Curve fitting

Typically, 50 cells/group for each donor/ acceptor set were bleached. Using a program written by one of us (J. L. Weaver), the bleaching curve data were extracted from the 2,000 points of the ACAS*.kpt data file. The data were smoothed using a five point weighted smoothing routine and were written as ASCII data files. These files were then used as input for the program NFIT (Island Products, Galveston, TX). Data were fit to a double exponential equation:

$$Y = A + B \cdot e^{-X/T1} + C \cdot e^{-X/T2}, \quad (3)$$

where Y is fluorescence intensity at time X, A is background fluorescence, B and C are the amplitudes of the two components decaying with the lifetimes T1 and T2, respectively. The program NFIT returns a fitted data set of 100 data points and the parameters of the fitted equation (A, B, T1, C, T2). These were imported into a spreadsheet program (Quattro Pro 3.0, Borland Inc., Scotts Valley, CA). The spreadsheet calculates an additional parameter, computed ratio (CR) for each curve:

$$CR = (B + C)/[(\Sigma\, Y_{\text{Fitted}}) - (A \cdot 100)] \quad (4)$$

The same spreadsheet also calculates the mean and the standard deviations for each parameter and performs a t-test for each pair (donor-only and donor + acceptor) of the average parameters. Finally, E is calculated using the CR values or the average of T1 and T2 weighted with their respective amplitude ratios:

$$E = 1 - CR(D + A)/CR(D), \quad (5)$$

and, based on (4),

$$E = 1 - T_{\text{avg}}(D)/T_{\text{avg}}(D + A), \quad (6)$$

where

$$T_{\text{avg}} = (T1 \times B + T2 \times C)/(B + C). \quad (7)$$

Eq. 7 is related to the fact that integration of the double exponential function yields the numerator of T_{avg}, which divided by the initial intensity will give the reciprocal of CR (just as integration of a single-exponential term divided by the initial amplitude gives the corresponding time constant).

The calculations for 2 × 50 cells take approximately 10 h on an AST Premium 386/SX computer (16 MHz) with an 80387SX math coprocessor, with the weighting option off, of the fitting program. A constant weighting was applied, as weighting (described in 12) of the squares of the residuals between experimental and fitted values did not improve fitting significantly but it substantially prolonged the analysis. The goodness of fitting was documented (see Results) by calculating X^2 as follows:

$$X^2 = \sum_i [(x_i - y_i)^2/y_i] \quad (8)$$

where x_i and y_i are the experimental and fitted values respectively. All the calculations were conducted using the same formula and calculating X^2 for 2,000 points, using the A, B, C, T1, and T2 parameters derived through fitting to generate the y_i values. Summation was done for 2,000-5 = 1,995 degree of freedom.

Flow cytometry

A FACScan (BD) flow cytometer was used to determine the staining of cells by the FITC or PE conjugated antibodies on the population level and as an alternate way of estimating (a mean) E. When necessary, compensation was set using the Calibrite calibration kit (BD) of FITC or PE stained microbeads. For donor quenching measurements, the sample pairs were run at various fluorescence amplification and compensation levels, including none, to avoid an artifactual quenching by over-compensation. Listmode data were collected and the FL1 (FITC) or FL2 (PE) distribution histograms, gated by forward and side scattering, analyzed using the Research Software package.

Staining of cells with antibodies

All the antibodies were added at saturating titers and incubated on ice, for 30 min. Two washes with PBS (phosphate buffered saline, pH 7.4) were applied between consecutive labelings and before fixation. Cells were fixed with 1% formaldehyde (prepared from paraformaldehyde in PBS) on ice for >1 h before scanning. Warming up of the cells to room temperature before fixation was avoided as it led to a rapid loss of labeling. Measurement of (fixed) samples older than two days was avoided and the FACScan distributions obtained immediately after labeling and just before bleaching were always compared.

RESULTS

Fig. 2 shows a typical bleaching curve, fitted to single and double-exponential decay curves. The double-exponential curve clearly fits the actual data more accurately: X^2 was ~1.4 when the bleaching curve of an OKT4-FITC labeled cell was fitted as double-exponential, and ~5.7 when it was assumed to be single-exponential. The X^2 values were <0.5 for fluorescent microbeads, and in the range of 0.015–0.025 for OKT4E labeled with FITC to a low FITC/protein ratio and bound to protein G-coupled Sepharose beads, with double exponential fitting. The latter values also increased 4–15 times on single-exponential fitting. In a semilogarithmic representation (inset of Fig. 2), fitting with a single exponential gives a straight line before diverging due to background fluorescence. A single-exponential fit with T_{avg} (calculated with the parameters obtained from the double-exponential fit) coincides with the previous, before coming to a different plateau.

The ratio of the amplitude values of the two components (B/C) was generally between 0.5–1.5, T1/T2 was ~0.2 and the background (A) was ~10% of the total intensity. T1 and T2, the reciprocal rate constants (of second order because oxygen radicals are also involved, see Discussion) in the two exponential terms are expected to increase and/or B/C decrease for $E > 0$. The ratio of extrapolated prebleach intensity and the integrated fluorescence (designated "CR" [computed ratio] in the tables below) is expected to decrease upon quenching.

The integrated fluorescence is expected to be a true measure of fluorophores present (5). We have evidence for this in our system from analyzing FITC-labeled beads at two clearly distinguishable distant focus levels

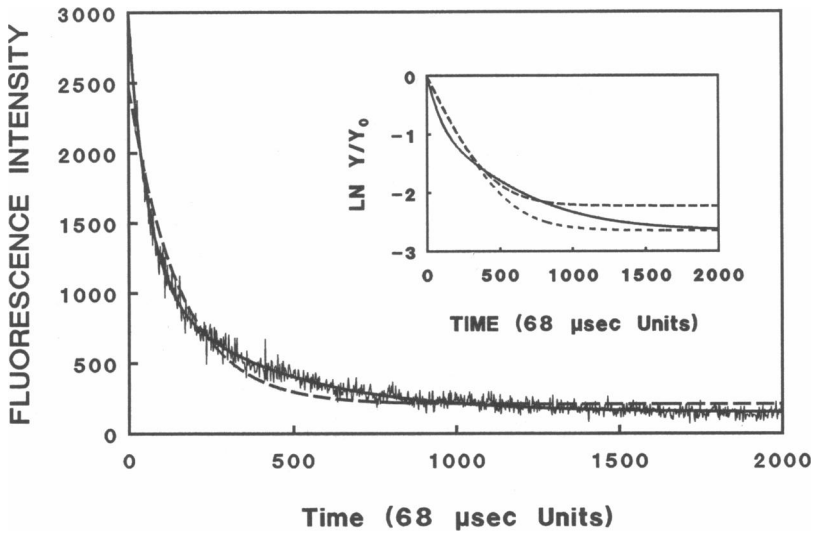

FIGURE 2 Photobleaching curves: actual data of OKT4-FITC-labeled HPB cells fitted with single (---) or double exponential (——) kinetics. Each data point represents bleaching for 68 µs units (see Methods). (*Inset*) natural logarithm of actual/initial fluorescence intensities of the same data, as a function of time. Double-exponential fitted data points (——); fitting the experimental data with single-exponential kinetics optimizing the time constant for the best fit (— —); single-exponential decay curve constructed with the initial intensity and T_{avg} from the double-exponential fit (--).

(at the outside rim or the uppermost point of the beads) where the initial intensities were different by ~20% (see Table 1). The integrated intensities were found not to differ significantly ($p > 0.05$) between the grossly altered focus levels, whereas all the E-related parameters had significantly different values. This experiment also pointed out focusing as a critical factor determining the error level of the measurements. The results obtained for a parallel pair of microbead samples mixed with Leu-3a-PE antibody were similar and also displayed FITC-to-PE pFRET (data not shown).

Table 2 summarizes the data obtained for pFRET between OKT4-FITC and Leu-3a-PE (specific for a two different epitopes on CD4). E between either OKT4-FITC and Leu-3a-PE or OKT4E-FITC and OKT4-PE, gave 17–20% values. Significantly lower (<4%) E values were obtained for pFRET between OKT4-FITC and Leu-5b-PE (αCD2; see Table 2). Very similar E values were calculated with the CR ratios and using the weighted average (T_{avg}) of T1 and T2. The individual time constants were increased to varying degrees for $E > 0$.

We investigated the possibility that a decreased initial intensity that could also be a nonspectroscopic consequence of acceptor binding (e.g., through an altered antigen conformation), might change the rate constants and CR in an artifactual manner, mimicking pFRET. The parameters used to calculate E (T_{avg} and CR) showed only a minor correlation with the labeling intensity of the cells, as demonstrated by the scattergrams generated for CR (or T_{avg}, not shown) and integrated fluorescence (see Fig. 3). A ~30% change in labeling (without energy transfer) would cause a 1–2% false shift in CR or T_{avg} and could be misinterpreted as a 1–2% E. Accordingly, when fluorescence intensity of the donor-only sample was experimentally decreased 30% by mixing Leu-3a-FITC with unlabeled antibody, no significant changes occurred in any of the parameters, as shown in Table 3.

The reproducibility of E values with our photobleaching method is demonstrated in Table 4. Repeated measurements of pFRET between two CD4 epitopes on the same fixed samples, and also between CD4 and CD3 on different batches of cells in separate experiments, gave nearly identical E values. The coefficients of variation were 10–14%. In the first case, the increments of T1 and T2 were 6.2 ± 3.2% and 8.9 ± 1.0%, respectively, while B/C decreased by 31.2 ± 2.6%.

A ~23% quenching of donor (OKT4-FITC) fluorescence by Leu-3a-PE was also demonstrated by flow cytometric analysis (Fig. 4). Quenching was barely detectable when Leu-4-PE (αCD3; or Leu-5b-PE [αCD2] or Leu-8-PE [directed against an adhesion molecule] data not shown) served as acceptor. All the other pFRET experiments run on the ACAS have also been controlled by running the same samples on the FACScan apparatus immediately before the bleaching experiment.

To check the distance sensitivity of the method, Leu-3a or Leu-3a-PE labeled cells stained with FITC-conjugated whole or F(ab')$_2$ secondary (αmouse IgG) antibody, respectively, were compared. The whole antibody is likely to carry the FITC moieties all over the F_c + $F(ab')_2$ fragments, probably having a larger average FITC-to-PE distance, as compared to when all the fluorophores are concentrated on the antigen-proximal $F(ab')_2$ fragments. Table 5 shows that E was 28% for

TABLE 1 Effect of focusing on energy transfer parameters

Parameter	Top focus[1]	Middle focus[2]	% Difference
T1[3]	112.3 ± 22.8	92.1 ± 14.2	−18.0[4]
T2	535.0 ± 114.0	420.0 ± 53.9	−21.5[4]
CR	0.065 ± 0.007	0.089 ± 0.008	+27.0[4]
$I(0)$[5]	2794 ± 504	3381 ± 397	+17.4[4]
I(int)[6]	43594 ± 11945	38484 ± 6956	−11.7[7]

[1]Average values ($N = 20$) ± standard deviation (SD) when focusing on the top of the FITC-labeled bead. [2]Values when focusing on the outside ring of the bead. [3]All T values are expressed in 68 μs units in all tables and figures. [4]Difference is significant at $p \ll 0.01$. [5]Extrapolated initial fluorescence intensity. [6]Total fluorescence intensity emitted during photobleaching. [7]Difference is not significant ($p > 0.05$).

TABLE 2 Energy transfer between T-cell antigens/epitopes

Parameter	Donor[1]	Donor + Acceptor[2]	E
	OKT4-FITC – Leu-3a-PE		
CR	0.121 ± 0.011	0.101 ± 0.010	16.5
T1	68.11 ± 10.81	97.37 ± 17.66	17.1
T2	355.6 ± 38.33	427.2 ± 87.49	
	OKT4E-FITC – OKT4-PE		
CR	0.111 ± 0.010	0.089 ± 0.007	19.8
T1	66.60 ± 7.70	76.20 ± 10.80	20.6
T2	370.6 ± 31.80	395.8 ± 45.10	
	OKT4-FITC – Leu-5b-PE		
CR	0.107 ± 0.007	0.103 ± 0.008	3.7
T1	61.70 ± 5.6	62.30 ± 5.7	4.5
T2	382.7 ± 23.4	393.1 ± 29.8	

Photobleaching FRET measurements. HPB cells were stained with FITC-conjugated first antibody, then labeled with unconjugated[1] or PE-conjugated[2] second antibody. E was calculated using the CR values (E = decrease of CR in the presence of the acceptor in %) or the average of T1 and T2 weighted with their respective amplitude ratios (T_{avg}, Eq. 6). The values are the mean ± SD for 50 cells/condition. The differences between the D and $D + A$ values are significant at $p < 0.01$ for all data pairs shown.

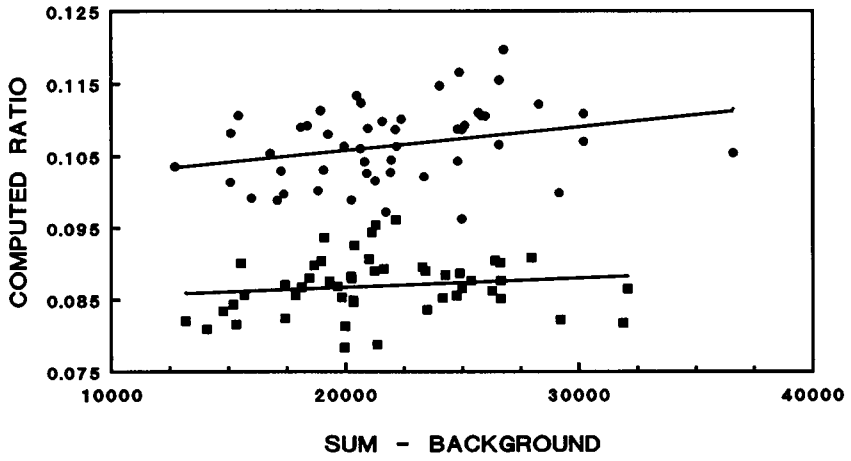

FIGURE 3 HPB cells stained with OKT4-FITC were labeled with unconjugated Leu-3a (•) or Leu-3a-PE (■). The results of the fitting of 50 cells/group photobleaching curves are represented as scattergrams: CR, calculated from the individual photobleaching curves is plotted as a function of the total integrated fluorescence of that particular cell (*curve*). The correlation coefficients for both data sets are below 0.3 (also for the scattergram of T_{avg}/total fluorescence, not shown). The slopes of the linear regression lines are <0.0003.

$F(ab')_2$-FITC and 14% when FITC was conjugated to the whole anti-mouse antibody.

Next, we compared pFRET between antibody FITC conjugates directed to different TcR epitopes and a CD3 epitope labeled with Leu-4-PE, on HPB-ALL. Surprisingly, as Table 6 shows, E was very high (~28%) between T40/25-FITC (directed against an idiotypic determinant of TcR α/β chain on these leukemia cells) and Leu-4-PE, and very low (E = 4%) between the TcR framework epitope and Leu-4-PE. Flow cytometric donor quenching measurements gave E values of 25.5% and 1.2%, respectively, for the above samples (histograms not shown). The amount of Leu-4-PE bound to the framework-specific αTcR-treated cells was ~40% lower than to T40/25-treated cells. A similar (~45%) decrease of CD3 labeling was observed on HPB cells when unconjugated framework-specific αTcR antibodies were added before or simultaneously with Leu-4-FITC or Leu-4-PE, as compared to cells stained only with the Leu-4-conjugates.

Possibilities of further improvement of sensitivity were raised comparing the utility of PE and TRITC as energy acceptors, as shown in Table 7. Cells labelled with Leu-4-FITC + αmouse-biotin were stained with (avidin-conjugates of) APC, PE or TRITC. The estimated sizes of the poor (for FITC fluorescence) energy acceptor APC and the excellent energy acceptor PE are 11 × 3 nm and 12 × 6 nm, respectively, both high

TABLE 3 Lack of correlation between pFRET parameters and donor concentration

Parameter	Donor	Donor + O[1]
CR	0.141	0.147
T1	49.83	47.44
T2	336.2	326.5

Cells were labeled with Leu-3a-FITC (D), or Leu-3a-FITC + Leu-3a ($D + O$) at a ratio to give a 30% decrease in the initial fluorescence intensity as measured by flow cytometry and the $B + C$ ratios. The differences between D and $D + O$ values are not significant ($p > 0.05$).

TABLE 4 Reproducibility of energy transfer parameters

	Exp. 1	Exp. 2	Exp. 3	Average ± S.D.
	Within batch variations[1]			
Energy transfer between OKT4-FITC and Leu-3a-PE:				
$E(CR)$	18.5	22.5	19.2	20.1 ± 2.1
$E(T_{avg})$	19.6	23.8	20.6	21.3 ± 2.2
	Batch to batch variations[2]			
Energy Transfer between OKT4-FITC and Leu-3a-PE:				
$E(CR)$	16.5	20.1	18.0	18.2 ± 1.8
$E(T_{avg})$	17.1	21.3	19.3	19.2 ± 2.1
Energy Transfer between OKT4-FITC and Leu-4-PE:				
$E(CR)$	9.2	7.5	6.8[3]	7.8 ± 1.2
$E(T_{avg})$	9.2	7.5	7.1[3]	7.9 ± 1.1

[1]HPB cells stained with OKT4-FITC and then with Leu-3a-PE or unconjugated Leu-3a. (This experiment was separate from that shown in Table 2.) Sets of cells (50/group) of the same fixed samples were bleached on three different days and E calculated using the CR or T_{avg} values. [2]Three different batches of HPB cells stained with OKT4-FITC were labeled with Leu-3a-PE (αCD4) (*middle panel*) or Leu-4-PE (αCD3) (*lower panel*). The donor-only samples were labeled in the second step with unconjugated antibody. The E values were determined based on the bleaching data using either the CR or the T_{avg} ratios. [3]These data were collected using the μsec mode (without delay between the time points).

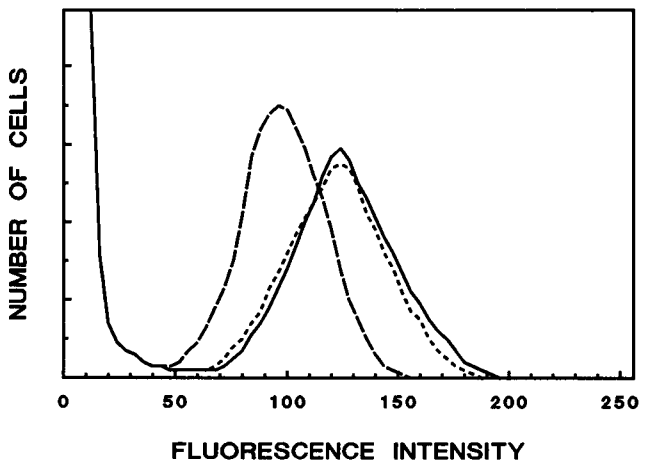

FIGURE 4 Flow cytometric analysis of average donor quenching. HPB cells stained with OKT4-FITC were labeled with unconjugated Leu-3a(αCD4) (——), Leu-3a-PE (---) or Leu-4-PE (αCD3) (· · ·). Analysis was gated by the small forward and side-scattering cells. E was calculated after a background FL1 value of the Leu-4-PE positive and OKT4-FITC negative subpopulation was subtracted from the FL1 means. No fluorescence compensation for FL1 was used.

molecular weight proteins considered cylindrical (13). E was ~32% when these cells were stained with TRITC-avidin and ~22% in the case of streptavidin-PE staining. The R_0 value (calculated as in [1]) was ~10 nm, assuming a ~160-kDa molecular weight. Thus, R_0 is higher for PE than the 5.6–7 nm value reported for TRITC (4).

DISCUSSION

The photobleaching FRET method introduced by Jovin and Arndt-Jovin (4) has been implemented on an ACAS instrument. The fidelity of acquired data is considerably increased as 2,000 time points are used to derive all the parameters of the bleaching curves. CCD cameras (used in the original method (4) have a much slower response and give less well resolved kinetics than the conventional photomultiplier tubes of the ACAS system we used. This advantage was exploited by the very precise curve-fitting of the bleaching kinetics. Surprisingly, the decay of fluorescence showed double, rather than single exponential kinetics (see Fig. 2). Our experimental evidence (Table 1) of the invariance of the area under the bleaching curve validates, in accordance with theory (5), the ratio of initial over integrated intensity (CR) as a true E-related parameter. We also showed that weighting the T values with the corresponding amplitudes (i.e., converting the double-exponential kinetics to a single exponential with initial and integral intensities equal to those of the double-exponential) gives nearly identical E values. The two calculations would not be expected to give the same values if bleaching had not been complete.

TABLE 5 **Whole or $F(ab')_2$ antibodies as donors**

Parameter	Donor[1]	Donor + acceptor[2]	E
	IgG		
CR	0.105	0.090	14.3
T1	71.9	85.6	14.4
T2	370.7	406.3	
	$F(ab')_2$		
CR	0.092	0.069	25.0
T1	76.5	96.3	31.6
T2	430.5	561.1	

Cells were labeled with Leu-3a (D^1) or Leu-3a-PE ($D + A^2$) and then stained with either intact αmouse IgG-FITC or $F(ab')_2$ αmouse IgG-FITC. The differences between D and $D + A$ values are significant with $p \ll 0.01$.

TABLE 6 **Energy transfer between epitopes of the T-cell receptor complex on HPB-ALL cells**

Parameter	D	$D + A$	E
	Energy transfer between T40/25-FITC and Leu-4-PE[1]		
CR	0.164	0.117	27.4[2]
T1	49.8	71.9	29.0[2]
T2	282.0	347.1	
	Energy transfer between αTcR-FITC and Leu-4-PE[3]		
CR	0.141	0.129	4.3[4]
T1	56.2	57.7	4.2[4]
T2	315.8	314.7	

[1]HPB-ALL T cell line labeled with T40/25-FITC (anti-idiotype) and either (D) unconjugated Leu-4 (anti-ϵ), or Leu-4-PE ($D + A$). [2]The difference between the means were significant at $p \ll 0.01$. [3]HPB-All cells labelled with αTcR-FITC (anti-α/β framework) and Leu-4 (D) or Leu-4-PE ($D + A$). Photobleaching FRET measurements were performed on 70 cells/condition. [4]The difference between the means of T1 and T2 were not significant ($p > 0.05$) and significant for *CR* ($p < 0.05$).

TABLE 7 **Comparison of PE and TRITC as acceptors**

Parameter	D + APC[1]	D + PE[2]	D + TRITC[3]	E1	E2
CR	0.094	0.075	0.065	20.2	30.9
T1	80.9	84.5	98.6	22.8	33.7
T2	403.0	467.4	517.4		

Cells were labeled with Leu-4-FITC then with αmouse-IgG-biotin. Aliquots were then stained with avidin conjugated to APC[1], PE[2] or TRITC[3]. The E1 and E2 values for E were calculated from the D + PE and D + TRITC data, respectively, comparing them to the D + APC data.

Using the data of Fig. 2, we showed that there was a ~25% difference between the E values calculated using CR or T_{avg} when bleaching was 80–85% in either D or $D + A$ samples. Thus, the coincidence of the E values obtained in both ways demonstrates that bleaching was complete in our experiments.

One of the possible explanations for double exponentiality could be that the different FITC moieties attached to the immunoglobulins are either not uniformly accessible to the diffusible components involved in the photobleaching process or have different intrinsic rates of photodestruction. However, prolongation of the photobleaching kinetics in the presence of the acceptor happened mainly through the changing B/C amplitude ratios. This fact also contradicts the possibility that the two exponential terms would come from the two isomeric forms present in some commercial FITC. The possibility that the diffusible reactants of bleaching (derived from dissolved oxygen, [14]) comprise more than one molecular species that are not available at the same abundance, seems unlikely for the same reason.

The double exponentiality of the photobleaching kinetics in our system is in contrast with what has been described earlier for fluorescent moieties bound to cells ([4 and recently 6] where the contribution of the second exponential term was found to be negligible) and fluorescein in solution (5). Because the temporal resolution of our measurements exceeded that of the earlier studies (4) (and for the initial period of bleaching, 5, and perhaps 6), it is possible that the actual kinetics were double-exponential also in those studies. More importantly, however, the actual illumination time upon bleaching in our case was 2,000 × 68 μs = 136 ms (collection of the 2,000 points took more than 40 s because of the 20-ms delay time between the points). Therefore, a T_{avg} value of 80 time units (on the instrument's scale) corresponds to ~6 ms, comparable to what was reported in an earlier study (5) and significantly shorter than the rates used in references 4 and 6 (up to seconds). Therefore, the mechanism of bleaching in our system could be different from that assumed to take place in the other related studies, perhaps involving the excited triplet states as well (14–15). At the incident power density used in our studies ($\sim 1.4 \times 10^3$ W/cm^2) a significant part of the excited state electrons are expected to accumulate in the triplet state, provided the medium is deoxygenated (14). Although this latter condition was not met in our system, it is conceivable that a significant number of triplet state molecules might be present throughout illumination, being continuously quenched or photoinactivated. The rate of intersystem crossing depends on the occupancy of excited singlet energy level and the emerging triplet state species are quickly engaged by the diffusional quencher molecular oxygen to generate highly reactive oxygen radicals or singlet oxygen with lifetimes in the μs range (15). Thus, it seems possible that the second exponential term of our decay curves reflects the photochemical destruction of the triplet state FITC moieties. In line with this hypothesis, the bleaching curve tends to assume single exponential kinetics (B/C decreases) when the laser intensity is decreased (data not shown).

We were concerned about the possibility that PE emission might sufficiently leak into channel FL1 to produce false changes in the kinetics, even though we could not detect any spillover by spectrofluorimetry. A major artifact of this origin was ruled out directly in the photobleaching experiments where E to the same (high surface density) acceptor was 29% from one donor and only 4% from another (Table 6). These values were similar to those obtained by flow cytometry. An artifact that might be related to the ~40% difference in Leu-4-PE labeling could not account for the above combined photobleaching and flow cytometric results. Furthermore, the E values obtained for pFRET between OKT4-FITC and Leu-3a-PE (both binding to CD4) were much higher than those calculated for pFRET between OKT4-FITC and Leu-4-PE (CD3), although the latter is present at a >2× higher concentration on the cell surface than Leu-3a (see Table 4). We also measured similar values of E between OKT4 and Leu3a or OKT4E (see Table 2), even though the FL2 intensity of Leu3a-PE was >3× higher than that of OKT4-PE (not shown), suggesting that the OKT4E epitope is actually closer than the gp120-binding Leu3a epitope, to the membrane-proximal OKT4. The third side of the triangle, the distance between OKT4E and Leu3a, appears to be much shorter than the Leu3a-to-OKT4 distance, according to our FACScan data (not shown).

At high acceptor concentrations, using cell lines, the background fluorescence of acceptor-only cells was higher than that of the unlabeled cells and this background fluorescence was bleachable (data not shown). Although this effect had no significant contribution to our results showing large E values (confirmed by flow cytometry), it is possible that our borderline (0–5%) results are afflicted by this effect. Therefore, the lower FACScan quenching values for pFRET between OKT4-FITC and Leu-4-PE (Fig. 4), or between αTcR-FITC and Leu-4-PE (Table 6), may be closer to reality than the values calculated from the bleaching experiments.

The application of PE as an energy acceptor (made possible by the near-complete overlap of its excitation spectrum with the emission spectrum of FITC, as pointed out in 7), has the advantage of a high apparent R_0 value (10 nm) and the availability of many commercial preparations (as opposed to TRITC-labeled antibodies). The size of PE may be of concern in flow cytometric

quenching studies (that measure just the initial intensity as opposed to the lifetime-related photobleaching method), because steric hindrance also might result in a decreased donor intensity. Any significant contribution of stearic hindrance to the apparent pFRET measured through the flow cytometric donor quenching assay was excluded because similar E values were obtained by the ACAS-based method. Also, changing the sequence of labeling with the donor and the acceptor did not alter the observed E values (data not shown). PE size can also be of advantage when intermolecular interaction are studied and PE can help bridge the distance between the particular epitopes labeled (suggested by data not shown).

Another possible artifact might occur when the cell surface density of acceptors is high enough to automatically invoke pFRET. Supposing a Poisson distribution for monomeric antigens on the (entire) cell surface, we estimate that this effect could be detectable when the acceptor density is more than 5×10^4 receptors/lymphocyte ($\sim$10-μm diameter). The dual detector image scans of the double-labeled (OKT4-FITC, Leu-4-PE) HPB cells (in conjunction with the experiment in Fig. 4 [data not shown]) showed a strong cocapping of the two antibodies, suggesting that the donor-acceptor pairs are confined to an area markedly smaller than the full surface of a cell. Therefore, it is possible that the *inter*molecular E values might have originated partly from this artifactual crowding of antigens.

The conversion of E to distances, although of doubtful significance in view of the size of the molecular components involved, is mechanisticly possible based on the R_0 = 10-nm value. Using the $E = R^{-6}/(R^{-6} + R_0^{-6})$ equation, E = 30% corresponds to 11.5 nm, 20% to 12.6 nm, 10% to 14.4 nm, and 5% to 16.3-nm donor-acceptor distance, respectively. To estimate experimentally the distance sensitivity of the method we used pFRET systems consisting of superimposed layers of antibodies recognizing each other, bound to cell surfaces. Based on the above calculations, the average D/A distance (between the $\sim$4 FITC and the $\sim$30 PE-chromophores, see ref. 13) may have changed from $\sim$13.5 to $\sim$11.7 nm, using $F(ab')_2$ fragments as donors, instead of whole antibodies.

CD3 is thought mainly to convey the signal (initiated by the engagement of TcR) to the cell interior (16–17). According to our data, the Leu-4 epitope on its ε chain may be juxtaposed with the antigen recognition motif of TcR, in accordance with the specific interaction described between the TcR β subunit and CD3 ε chain (17). The above pFRET data, together with the significantly decreased Leu-4 labeling of αTcR-treated cells ($\sim$35%; $\sim$42 and $\sim$47% for HPB cells stained with Leu-4-PE or another PE-labeled ε chain-specific clone, UCHT1, respectively, data not shown) can be interpreted in two ways. The first interpretation is that αTcR alters CD3 conformation so that Leu-4 will bind with less avidity. The second is that the two CD3 ε chains thought to participate in the complex (16–17) are not equivalent in their position relative to TcR α/β and one of them may be completely blocked by the framework-specific αTcR, with the other being too far away to give energy transfer. This latter possibility would be compatible with the extent of decrease in Leu-4-binding after TcR-treatment and with the finding that αTcR added after Leu-4-FITC or PE did not change staining (data not shown). Because the two ε chains of the TcR/CD3 complex appear to interact with each other (for FRET data see 16), we speculate that one of the chains occupies a more distal position, relative to TcR β. This conclusion is somewhat mitigated if the single donor-multiple acceptors approximation (18) is applied to our systems. E would be expected to decrease from $\sim$28% to 17% as a result of the elimination of one epsilon binding site by αTcR, as opposed to the change from 28% to 4% actually observed.

The bleaching method should always be used in conjunction with a dual detection method (flow cytometric analysis or two-color image scans), to determine the FL2 distribution of the FL1-positive cells (approximately half the αCD3-FITC labeled HPB cells would bind αCD4-PE, e.g., requiring the scanning of a larger number of cells by the ACAS and the construction of scattergrams as shown in Fig. 3). The number of cells scanned by the ACAS method is far lower than what is feasible by flow cytometric methods. Therefore, it is possible, though not likely in our experience, that a sample of 50 cells may not be representative, comprising perhaps mostly of a specific subpopulation of donor + acceptor positive cells (not a consideration for the data presented here). Performing the same experiment on several batches of cells or bleaching FACS-separated samples can eliminate this problem. Another source of cell-to-cell diversity is the inherent variability of the parameters analyzed, even in the case of the microbeads. The much better fit in case of the Sepharose-bound IgG with low F/P ratio (see Results) suggests that the various FITC moieties may exhibit different bleaching kinetics. The data presented here demonstrate for the first time the routine applicability of the ACAS apparatus for pFRET measurements, the possibility of using PE as an energy acceptor and the feasibility of pFRET measurements also on HPB cells (that carry smaller numbers of cell surface antigens than the cell lines studied by FRET methods earlier). TRITC, when sufficient quantities of purified antibody are available for labeling may still be the acceptor of choice, especially

when conformational changes are to be detected, in view of the comparative data in Table 7.

We have recently found that bleaching in the μs scale (without the 20 ms delay periods between pulses) diminishes the background problem mentioned above. The E values obtained were invariant to the longevity of the delay time, as shown in Table 4 (and according to parallel experiments performed on the same samples in both time modes [data not shown]). This modification will also greatly enhance the efficiency of this technique, because bleaching of ~50 cells can be accomplished within less than an hour, making the scanning of live cells feasible and also eliminating the problem of occasional cell movement during photobleaching. At present, using the longer bleaching routine, we get reproducible and consistent results at a rate of one pair of samples a day, on human peripheral blood cells.

We are grateful for discussions with Prof. L. Tròn, University Med School of Debrecen, Hungary, at the initial phase of this project. We would like to thank Drs. J. R. Lakowicz and H. Malak (University of Maryland, Baltimore, MD) for their help in the calculation of R_0; Dr. P. Rao (Ortho Diagnostics Inc., Raritan, NJ) for a gift of OKT4E and Dr. D. B. Tse (North Shore University Hospital-Cornell University Medical College, Manhasset, NY) for HPB-ALL and T40/25-FITC. We would also like to thank Dr. L. Reinisch (Vanderbilt University, Nashville, TN) for helpful discussions during the preparation of this manuscript.

Note added in proof: The WT31 antibody was recently shown (Salmeròn, A.F., et al., *J. Immunol.* 147:3047, 1991) to bind to a combination epitope involving $CD3_\epsilon$, rather than to TcR α/β (as previously thought). This result seems to be in agreement with our conclusions.

Received for publication 9 September 1991 and in final form 11 November 1991.

REFERENCES

1. Szöllösi, J., S. Damjanovich, S. A. Mulhern, and L. Tròn. 1987. Fluorescence energy transfer and membrane potential measurements monitor dynamic properties of cell membranes: a critical review. *Prog. Biophys. Mol. Biol.* 49:65–87.
2. Tròn, L., J. Szöllösi, S. Damjanovich, S. H. Helliwell, D. J. Arndt-Jovin, and T. M. Jovin. 1984. Flow cytometric measurements of fluorescence resonance energy transfer on cell surfaces. Quantitative evaluation of the transfer efficiency on a cell-by-cell basis. *Biophys. J.* 45:939–946.
3. Matkò, J., J. Szöllösi, L. Tròn, and S. Damjanovich. 1988. Luminescence spectroscopic approaches in studying cell surface dynamics. *Q. Rev. Biophys.* 21:479–544.
4. Jovin, T. M., and D. J. Arndt-Jovin. 1989. FRET microscopy: digital imaging of fluorescence resonance energy transfer. Application in cell biology. *In* Cell Structure and Function by Microspectrofluorimetry. E. Kohen, J. S. Ploem, and J. G. Hirschberg, editors. Academic Press, Orlando, FL. 99–117.
5. Hirschfeld, T. 1976. Quantum efficiency independence of the time integrated emission from a fluorescent molecule. *Appl. Optics.* 15:3135–3139.
6. Kubitscheck, U., M. Kircheis, R. Schwitzer-Stenner, W. Dreybrodt, T. M. Jovin and I. Pecht. 1991. Fluorescence resonance energy transfer on single living cells. Application to binding of monovalent haptens to cell-bound immunoglobulin E. *Biophys. J.* 60:307–318.
7. Chapple, M. R., G. D. Johnson and R. S. Davidson. 1988. Fluorescence quenching of fluorescein by R-phycoerythrin. A pitfall in dual fluorescence analysis. *J. Immunol. Methods.* 111:209–217.
8. T. Kieber-Emmons, B. A. Jameson, and W. J. W. Morrow. 1989. The gp120-CD4 interface: structural, immunological and pathological considerations. *Biochim. Biophys. Acta.* 989:281–300.
9. Chuck, R. S., C. R. Cantor, and D. B. Tse. 1990. CD4-T-cell antigen receptor complexes on human leukemia T cells. *Proc. Natl. Acad. Sci. USA.* 87:5021–5025.
10. Mizukami, T., T. R. Fuerst, E. A. Berger, and B. Moss. 1988. Binding region for human immunodeficiency virus (HIV) and epitopes for HIV-blocking monoclonal antibodies of the CD4 molecule defined by site-directed mutagenesis. *Proc. Natl. Acad. Sci. USA.* 85:9273–9277.
11. Suzaki, Y., and A. Tachibana. 1975. Measurement of the μm sized radius of Gaussian laser beam using the scanning knife-edge. *Appl. Optics.* 14:2809–2811.
12. Grinvald, A., and I. Z. Steinberg. 1974. On the analysis of fluorescence decay kinetics by the method of least squares. *Anal. Biochem.* 59:583–598.
13. Glazer, A. N., and L. Stryer. 1983. Fluorescent tandem phycobiliprotein conjugates. *Biophys. J.* 43:383–386.
14. Lanni, F., and B. R. Ware. 1981. Intensity dependence of fluorophore photobleaching by a stepped-intensity slow-bleach experiment. *Photochem. Photobiol.* 34:279–281.
15. Vanderkooi, J. M., G. Maniara, T. J. Green, and D. F. Wilson. 1987. An optical method for measurement of dioxygen concentration based upon quenching of phosphorescence. *J. Biol. Chem.* 262:5476–5482.
16. de la Hera, A., U. Müller, C. Olsson, S. Isaaz, and A. Tunnacliffe. 1991. Structure of the T Cell Antigen Receptor (TCR): Two CD3e Subunits in a Functional TCR/CD3 Complex. *J. Exp. Med.* 173:7–17.
17. Tan, L., J. Turner, and A. Weiss. 1991. Regions of the T cell receptor α and β chains that are responsible for interaction with CD3. *J. Exp. Med.* 173:1247–1256.
18. Gennis, R. B., and C. R. Cantor. 1972. Use of nonspecific dye labeling for singlet energy-transfer measurements in complex systems. A simple model. *Biochemistry.* 11:2509–2517.